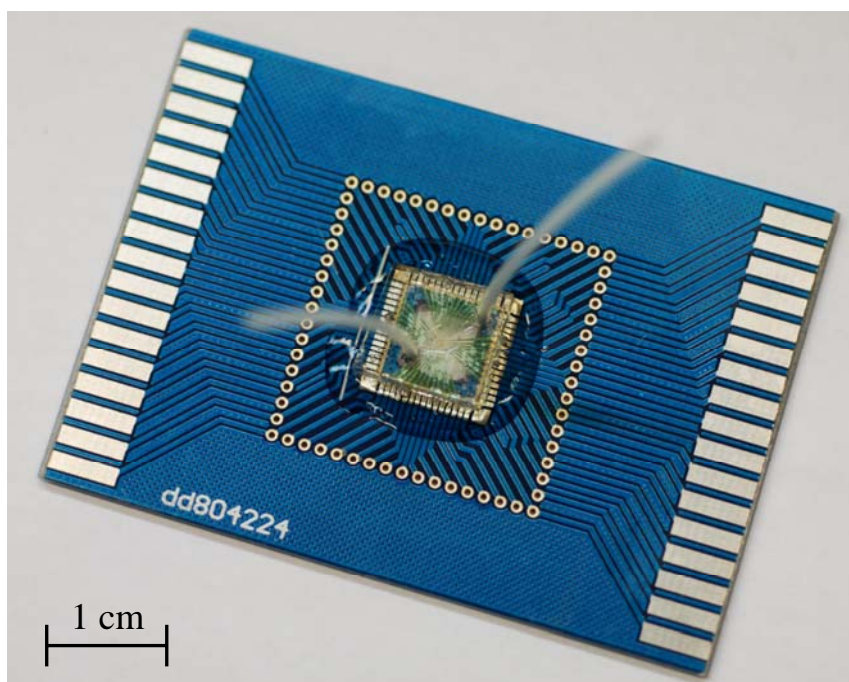


1 **The construction of a positive dielectrophoresis-enabled cell**
2 **arraying-assisted electroporation (CAE) chip for selective**
3 **electroporation**

4 Youchun Xu, Huanfen Yao, Lei Wang, Wanli Xing and Jing Cheng

5 **Fig. S1**

6 The full view of assembled device



7

8

9 The assembled device, which has a sandwich structure from bottom to top: printed circuit
10 board, glass chip, polymethyl methacrylate (PMMA) spacer and indium tin oxides (ITO)
11 covered slide. Extra tubes are connected with inlet and outlet of device for medium infusing.

12

13

14

15

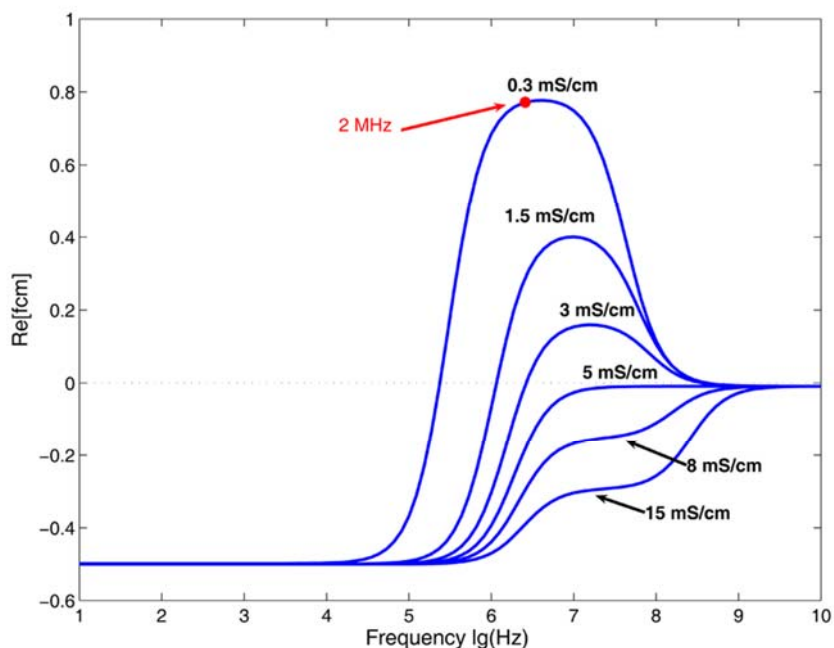
16

17

18

1 **Fig. S2**

2 The simulations of the real part of the Clausius-Mossotti factor (f_{CM})



3

4 The real part of the Clausius-Mossotti factor f_{CM} as a function of frequency for mammalian cells
5 using a single-shell model. The typical parameters for the single-shell model of mammalian
6 cells were given by Oblak¹. Each curve was calculated for a different medium conductivity: σ_m
7 = 0.3, 1.5, 3, 5, 8 and 15 mS/cm. The typical conductivity of cell culture medium is 15 mS/cm,
8 in which cells always endure negative dielectrophoretic force in non-uniform electric field. The
9 optimal parameters for pDEP is chosen as: 0.3 mS/cm and 2 MHz in our experiment, which is
10 consistent with the simulation result.

11

12

13

14 **Reference**

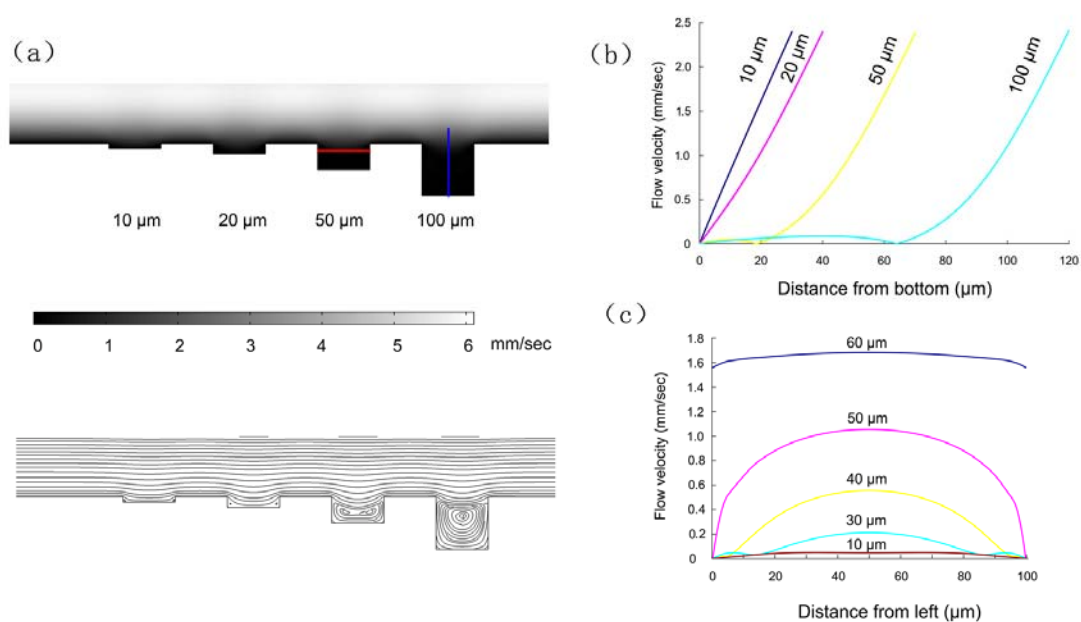
15 1 J. Oblak, D. Krizaj, S. Amon, A., Macek-Lebar and D. Miklavcic, Feasibility study for cell
16 electroporation detection and separation by means of dielectrophoresis. *Bioelectrochemistry*
17 2007, 71, 164-171

18

19

1 **Fig. S3**

2 Flow profile from numerical simulations



3

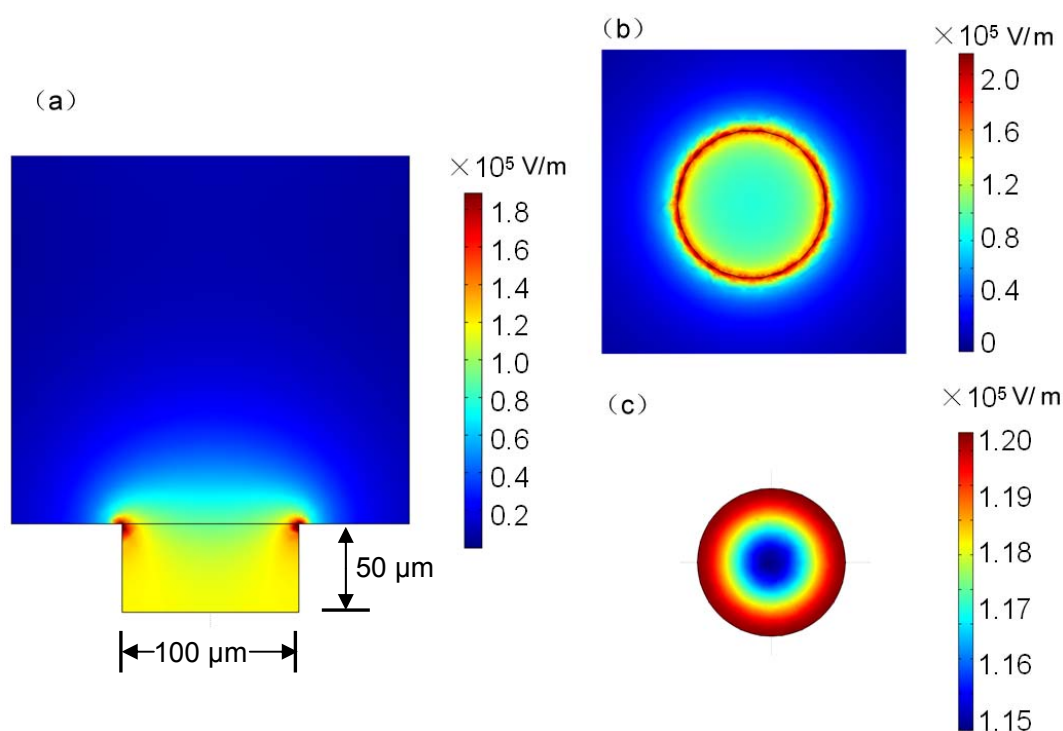
4 The flow field in a micro-well was simulated by a 2D model with the commercial software
5 (COMSOL Multiphysics 3.5) to find the optimal geometry of micro-well. (a) Simulation of flow
6 velocity inside the micro-wells (Diameter = 100 μm) with different depths (10, 20, 50, and 100
7 μm). The channel flow speed was set at 4 mm/sec from left to right. Velocity contours and
8 streamline patterns for micro-wells are given respectively. High micro-well depths (25 and 50
9 μm) show major recirculation areas; the direction of the local velocity near the base of these
10 grooves is opposite to the mainstream fluidic flow. (b) Flow field at the central line (the blue line
11 indicated in (a)) of each micro-well was acquired from the simulation result, and then a plot of
12 flow velocity vs. the distance from the bottom of each micro-well was presented. The
13 micro-well with 50 μm depth shows significant low flow velocity area (0 to 20 μm distance from
14 bottom), which matches with the size of mammalian cell. Thus, 50 μm was chosen as the
15 optimal depth of micro-well. (c) Flow field at the different distance from bottom (the red line
16 indicated in (a)) of the micro-well (50 μm depth) was acquired from the simulation result, and
17 then a plot of flow velocity vs. the distance from left wall of micro-well was presented. Flow
18 velocity is low in the bottom of the micro-well, especially in the corner.

19

20

1 **Fig. S4**

2 Electric field profile from numerical simulations



3

4 The electric field in a micro-well was simulated by a 3D model with the commercial software
5 (COMSOL Multiphysics 3.5) using the electrostatic form of Poisson's equation. The electric
6 signal was applied as 20 V, and the parameters of buffer were set as: conductivity of 3×10^{-2}
7 S/m, relative permittivity of 81. (a) Schematic cross-section of the micro-well showing electric
8 field intensity, with a rain-bow plot showing the magnitude of the electric field squared;
9 proportional to the DEP potential energy. The electric field intensity in the micro-well is
10 non-uniform and higher than outside. Cells are trapped by positive dielectrophoresis (pDEP) in
11 regions of high field strength and move towards micro-well. Moreover, the electric field
12 intensity in the micro-well is also non-uniform, highest in the top corner of the micro-well. (b)
13 The vertical view of electric field intensity on the top of the micro-well (50 μm distance from
14 bottom). (c) The vertical view of electric field intensity on the bottom of the micro-well (10 μm
15 distance from bottom). Cells in the micro-well are apt to position in the corner.

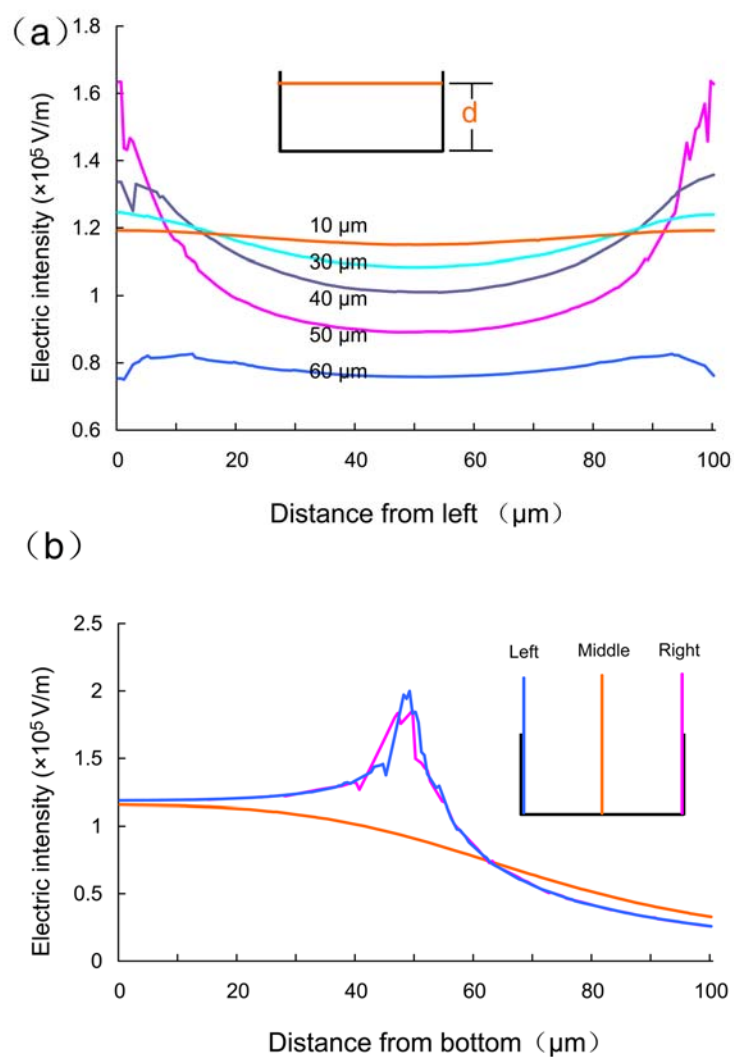
16

17

18

1 **Fig. S5**

2 Calculated electric field in the micro-well



3

4 Electric field at different positions was acquired and calculated from the simulation result

5 (shown in Supplementary Figure 2). (a) Electric field at the central line of different level ($d = 10$,

6 30, 40, 50 and 60 μm distance from bottom of the micro-well) was plotted vs. the distance from

7 left wall of micro-well. (b) Electric field at the central line at different positions was plotted vs.

8 the distance from the bottom of micro-well. These curves clearly show that electric field

9 intensity in the micro-well is basically higher than outside, especially in the corner.

10

11

12

13